

Adipocyte Enhancer-Binding Protein 1 (AEBP1) (a Novel Macrophage Proinflammatory Mediator) Overexpression Promotes and Ablation Attenuates Atherosclerosis in *ApoE*^{-/-} and *LDLR*^{-/-} Mice

Oleg Bogachev,* Amin Majdalawieh,*[†] Xuefang Pan,* Lei Zhang, and Hyo-Sung Ro

Department of Biochemistry and Molecular Biology, Faculty of Medicine, Dalhousie University, Halifax, Nova Scotia, Canada;

[†]current affiliation: Department of Biology, Chemistry and Environmental Sciences, Faculty of Arts and Sciences, American University of Sharjah, Sharjah, United Arab Emirates

Atherogenesis is a long-term process that involves inflammatory response coupled with metabolic dysfunction. Foam cell formation and macrophage inflammatory response are two key events in atherogenesis. Adipocyte enhancer-binding protein 1 (AEBP1) has been shown to impede macrophage cholesterol efflux, promoting foam cell formation, via peroxisome proliferator-activated receptor (PPAR)- γ 1 and liver X receptor α (LXR α) downregulation. Moreover, AEBP1 has been shown to promote macrophage inflammatory responsiveness by inducing nuclear factor (NF)- κ B activity via I κ B α downregulation. Lipopolysaccharide (LPS)-induced suppression of pivotal macrophage cholesterol efflux mediators, leading to foam cell formation, has been shown to be mediated by AEBP1. Herein, we showed that *AEBP1*-transgenic mice (*AEBP1*^{TG}) with macrophage-specific AEBP1 overexpression exhibit hyperlipidemia and develop atherosclerotic lesions in their proximal aortas. Consistently, ablation of *AEBP1* results in significant attenuation of atherosclerosis (males: 3.2-fold, $P = 0.001$ (*en face*), 2.7-fold, $P = 0.0004$ (aortic roots); females: 2.1-fold, $P = 0.0026$ (*en face*), 1.7-fold, $P = 0.0126$ (aortic roots)) in the *AEBP1*^{-/-}/*low-density lipoprotein receptor (LDLR)*^{-/-} double-knockout (KO) mice. Bone marrow (BM) transplantation experiments further revealed that *LDLR*^{-/-} mice reconstituted with *AEBP1*^{-/-}/*LDLR*^{-/-} BM cells (*LDLR*^{-/-}/*KO*-BM chimera) display significant reduction of atherosclerosis lesions (*en face*: 2.0-fold, $P = 0.0268$; aortic roots: 1.7-fold, $P = 0.05$) compared with control mice reconstituted with *AEBP1*^{+/+}/*LDLR*^{-/-} BM cells (*LDLR*^{-/-}/*WT*-BM chimera). Furthermore, transplantation of *AEBP1*^{TG} BM cells with the normal *apolipoprotein E (ApoE)* gene into *ApoE*^{-/-} mice (*ApoE*^{-/-}/*TG*-BM chimera) leads to significant development of atherosclerosis (males: 2.5-fold, $P = 0.0001$ (*en face*), 4.7-fold, $P = 0.0001$ (aortic roots); females: 1.8-fold, $P = 0.0001$ (*en face*), 3.0-fold, $P = 0.0001$ (aortic roots)) despite the restoration of ApoE expression. Macrophages from *ApoE*^{-/-}/*TG*-BM chimeric mice express reduced levels of PPAR γ 1, LXR α , ATP-binding cassette A1 (ABCA1) and ATP-binding cassette G1 (ABCG1) and increased levels of the inflammatory mediators interleukin (IL)-6 and tumor necrosis factor (TNF)- α compared with macrophages of control chimeric mice (*ApoE*^{-/-}/*NT*-BM) that received AEBP1 nontransgenic (*AEBP1*^{NT}) BM cells. Our *in vivo* experimental data strongly suggest that macrophage AEBP1 plays critical regulatory roles in atherogenesis, and it may serve as a potential therapeutic target for the prevention or treatment of atherosclerosis.

© 2011 The Feinstein Institute for Medical Research, www.feinsteininstitute.org

Online address: <http://www.molmed.org>

doi: 10.2119/molmed.2011.00141

INTRODUCTION

Atherosclerosis is a killer disease responsible for >50% of deaths in the developed world (1,2). Although some researchers seem to focus on atherosclerosis

as either a metabolic/lipid disorder or an inflammatory disorder, there is a general consensus among most investigators that atherosclerosis is a complex disease involving both metabolic and inflamma-

tory dysfunctions. Once fully differentiated in the intima, macrophages express a wide range of scavenger receptors that allow internalization of modified low-density lipoprotein (LDL). Lipid accumulation in macrophages leads to the activation of signaling pathways that involve activation of peroxisome proliferator-activated receptor (PPAR)- γ 1 and liver X receptor α (LXR α), nuclear receptors that function as transcription factors controlling macrophage cholesterol homeostasis (3–7). Ligand-bound activated PPAR γ 1 and LXR α are syner-

*OB, AM, and XP contributed equally to this work.

Address correspondence and reprint requests to Hyo-Sung Ro, Department of Biochemistry and Molecular Biology, Dalhousie University, Sir Charles Tupper Medical Building, 5850 College Street, Halifax, NS, B3H 1X5 Canada. Phone: 902-494-2367; Fax: 902-494-1355; E-mail: hsro@dal.ca.

Submitted April 18, 2011; Accepted for publication June 9, 2011; Epub (www.molmed.org) ahead of print June 14, 2011.

gistically implicated in the transactivation of several genes for which products are critically involved in mediating macrophage cholesterol efflux and initiating reverse cholesterol transport. Genetic defects or pharmacological inhibition of any component of the macrophage cholesterol efflux pathway leads to an imbalance in cholesterol homeostasis. This result eventually leads to massive accumulation of lipids in the cytoplasmic compartment of macrophages, which acquire a foamy appearance and transform into lipid-engorged foam cells, a hallmark of fatty streak and atherosclerotic lesion formation. Because atherosclerosis is a multigenic disease, understanding the roles and expression patterns of genes with known and unknown functions is critical in understanding the molecular mechanisms underlying atherogenesis.

Adipocyte enhancer-binding protein 1 (AEBP1) is a ubiquitously expressed transcriptional repressor for which expression is highest in white and brown adipose tissues, liver, lung, spleen and brain (8). Recently, AEBP1 was shown to be abundantly expressed in primary macrophages and macrophage cell lines (9–11). We demonstrated that AEBP1 represses the expression of PPAR γ 1 and LXR α in a dose-dependent, DNA binding-dependent fashion, which is accompanied by concurrent repression of major cholesterol efflux mediators (for example, ATP-binding cassette A1 (ABCA1), ATP-binding cassette G1 (ABCG1) and apolipoprotein [Apo]-E), leading to foam cell formation (9). AEBP1 was also shown to promote macrophage inflammatory responsiveness by inducing nuclear factor (NF)- κ B activity via I κ B α -negative regulation through protein-protein interaction (10). These experimental findings strongly suggest that AEBP1 may exert potent atherogenic effects *in vivo*. We hypothesize that AEBP1 overexpression promotes lesion formation, while AEBP1 ablation attenuates lesion formation in *ApoE*^{-/-} and *low-density lipoprotein receptor (LDLR)*^{-/-} murine models of atherosclerosis.

In this study, ablation of AEBP1 (12) in the *LDLR*^{-/-} mice (*AEBP1*^{-/-}*LDLR*^{-/-}), *LDLR*^{-/-} mice receiving *AEBP1*^{-/-}*LDLR*^{-/-} bone marrow (BM) cells and *ApoE*^{-/-} mice receiving BM cells from *AEBP1*^{TG} mice (13) that overexpress AEBP1 in macrophages were used as invaluable *in vivo* tools to assess the involvement of AEBP1 in atherosclerotic lesion formation. Remarkably, AEBP1 ablation significantly reduced atherosclerosis in *LDLR*^{-/-} mice challenged with an atherogenic diet. Moreover, *LDLR*^{-/-} mice receiving BM cells from *LDLR*^{-/-}/*AEBP1*^{-/-} mice exhibited marked reduction of atherosclerosis. In contrast, transplantation of BM cells with the wild-type *ApoE* gene from *AEBP1*^{TG} mice into *ApoE*^{-/-} mice did not ameliorate atherosclerosis; rather, it led to enhanced lesion formation. Collectively, our findings clearly demonstrate that AEBP1 manifests itself as a potent pro-atherogenic factor. We anticipate that AEBP1 may serve as a likely molecular target for developing novel therapeutic strategies for the prevention or treatment of atherosclerosis.

MATERIALS AND METHODS

Animal Experiments

AEBP1^{-/-} mice (12) were bred with *LDLR*^{-/-} mice (The Jackson Laboratory, Bar Harbor, ME, USA). Intercrosses of *AEBP1*^{-/-}/*LDLR*^{-/-} mice yielded offspring that entered the study. Genotyping for AEBP1 and LDLR was performed by polymerase chain reaction (PCR). For analysis of atherosclerosis, mice were fed an atherogenic diet (high-cholesterol diet [HCD]) (40 kcal % fat, 1.25% cholesterol, 0% cholic acid; D12108C; Research Diets, New Brunswick, NJ, USA) beginning at 3 wks of age for a period of 13 wks. For high-fat diet (HFD) feeding experiments, mice were fed HFD (45 kcal % fat, 0.05% cholesterol, 0% cholic acids; D12451; Research Diets) beginning at 3 wks of age.

BM cells were collected from the femurs and tibias of donor mice. Total T cells were depleted using CD90.2 microbeads (EasySep, StemCell Tech-

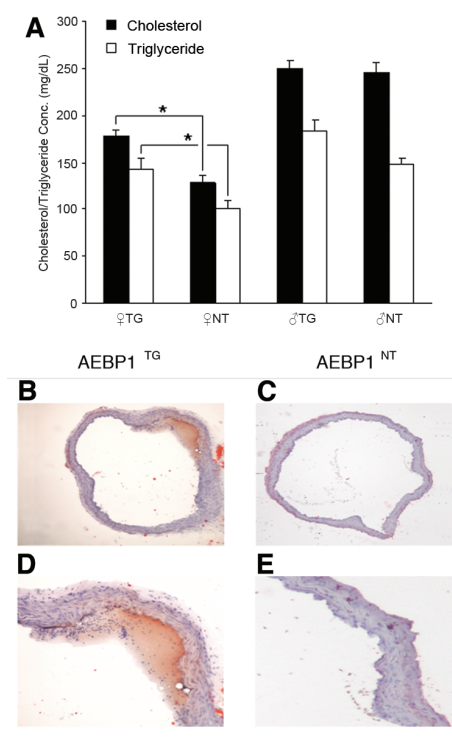


Figure 1. AEBP1 promotes diet-induced hyperlipidemia and atherosclerosis in mice. (A) Whole blood samples were obtained from 32-wk-old, HFD-fed *AEBP1*^{TG} and *AEBP1*^{NT} mice to measure total cholesterol and triglyceride serum levels by gas chromatograph. Concentration (Conc.) of total cholesterol and triglycerides is expressed as mg/dL, and data are demonstrated as mean \pm SEM (n = 3–5). Statistical significance was determined relative to cholesterol or triglyceride serum level in *AEBP1*^{NT} mice for each gender. To assess lipid-filled lesion formation, aortic cryosections obtained from 12- and 32-wk-old, chow- and HFD-fed *AEBP1*^{TG} and *AEBP1*^{NT} mice were stained with ORO. Representative images of ORO-stained aortic cryosections from 32-wk-old, HFD-fed *AEBP1*^{TG} (B, D) and *AEBP1*^{NT} (C, E) females are shown at 100 \times (B, C) and 400 \times (D, E) magnification. A total of 3–35 mice per group were examined (refer to Table 1 for more details).

nologies, BC, Canada). Recipient *ApoE*^{-/-} (The Jackson Laboratory) and *LDLR*^{-/-} mice at the age of 8–10 wks were lethally irradiated (800 rad) and then injected with BM cells (2×10^6) through the tail vein. Two weeks after BM transplanta-

tion, mice were placed on an atherogenic diet for 16 wks and then sacrificed to isolate BM cells and spleens for real-time PCR.

Mice were deeply anesthetized with isoflurane, and blood was obtained by intracardiac puncture. Plasma cholesterol and triglyceride levels were determined by enzymatic assays (Roche Diagnostics, Laval, QC, Canada, and Sigma, St. Louis, MO, USA). The aortas and hearts were isolated for *en face* and aortic root atherosclerotic lesion analysis.

All animal experiments were performed according to procedures approved by the Institutional Animal Care Committee (Carleton Animal Care Facility, Dalhousie University, Halifax, NS, Canada). Age-matched mice were kept on a 12-h light cycle.

Atherosclerotic Lesion Analysis

For *en face* analysis, aorta isolation and detection of atherosclerotic lesions using sudan IV were performed as previously described (14), and images were captured with a PixeLINK PL-A686C camera attached to a Leica MZ6 dissecting microscope. Aortic cryosection analysis of atherosclerotic lesions in the proximal aortic root was performed as previously described (15), and photomicroscopy was performed on a Nikon Eclipse E600 microscope attached to a Nikon Coolpix 990 camera. In all cases, the percentage of stained lesion size was determined using ImageJ analysis software.

Immunohistochemistry for Aortic Cryosection

The hearts were harvested from *AEBP1*^{+/+}/*LDLR*^{-/-} and *AEBP1*^{-/-}/*LDLR*^{-/-} mice fed an atherogenic diet for 13 wks and were fixed in 10% buffered formalin overnight. The next day, the hearts were put in 0.02% sodium azide in phosphate-buffered saline. Consecutive 5- μ m cryosections of the heart from the aortic sinus to the beginning of the aortic arch were subjected to immunohistochemistry using rat anti-mouse F4/80 (Abcam, San Francisco, CA, USA) for macrophage detection, rat anti-mouse CD106 for vascu-

Table 1. Effect of *AEBP1* genotype, gender, age and diet on atherosclerotic lesion formation in mice.

Gender and genotype	Age (wks)	Diet	Total number of mice (n)	Lesion prevalence (%)
F <i>AEBP1</i> ^{TG}	32	Chow	18	—
M <i>AEBP1</i> ^{TG}	32	Chow	9	—
F <i>AEBP1</i> ^{NT}	32	Chow	8	—
M <i>AEBP1</i> ^{NT}	32	Chow	8	—
F <i>AEBP1</i> ^{TG}	12	HFD	8	50 (4 of 8)
M <i>AEBP1</i> ^{TG}	12	HFD	8	50 (4 of 8)
F <i>AEBP1</i> ^{NT}	12	HFD	9	—
M <i>AEBP1</i> ^{NT}	12	HFD	8	—
F <i>AEBP1</i> ^{TG}	32	HFD	35	94 (32 of 35)
M <i>AEBP1</i> ^{TG}	32	HFD	32	72 (23 of 32)
F <i>AEBP1</i> ^{NT}	32	HFD	32	—
M <i>AEBP1</i> ^{NT}	32	HFD	29	—

lar cell adhesion molecule 1 (VCAM-1) detection (BD Pharmingen, San Diego, CA, USA), rat anti-mouse CD3 for T-cell detection (BD Pharmingen) and normal rat IgG as a negative control.

Macrophage Isolation

Macrophages were isolated from the spleen using EasySep specific antibodies and tiny fluorescence-activated cell sorter (FACS)-compatible magnetic nanoparticles in a column-free magnetic system (StemCell Technologies). Purity (~98%) was confirmed by flow cytometry.

RNA and Protein Analysis

Total RNA was isolated from the spleen and BM cells using TRIZOL (Invitrogen, Burlington, ON, Canada) and was then reverse-transcribed into cDNA using an iScript cDNA synthesis kit (Bio-Rad, Mississauga, ON, Canada). PCR was performed using a CFX96 optical reaction module (Bio-Rad). Protein extraction and immunoblotting were performed as previously described (13).

Statistical Analysis

Group means were compared with a Student *t* test. A probability value of ≤ 0.05 was considered statistically significant. All data are reported as mean \pm standard error of the mean (SEM) as indicated.

All supplementary materials are available online at www.molmed.org.

RESULTS

AEBP1^{TG} Mice Exhibit Signs of Atherosclerotic Lesion Formation in a Gender-Influenced Manner

The fact that *AEBP1* overexpression causes cholesterol homeostasis imbalance in macrophages (9,11) prompted us to examine the serum lipid profile in *AEBP1*^{TG} mice that overexpress *AEBP1* in macrophages (9). Serum samples obtained from 32-wk-old, HFD-fed *AEBP1*^{TG} females had significantly higher serum cholesterol and triglyceride levels than samples from *AEBP1*^{NT} females (cholesterol, 179 ± 6.2 and 128 ± 7.3 mg/dL, $P < 0.05$; triglyceride, 143 ± 12.3 and 100 ± 9.3 mg/dL, $P < 0.05$, respectively). Although *AEBP1*^{TG} males have higher serum cholesterol and triglyceride levels than *AEBP1*^{NT} males, this difference did not reach statistical significance (Figure 1A). We have previously shown that while triglyceride serum levels are significantly lower in *AEBP1*^{-/-} mice compared with *AEBP1*^{+/+} mice, cholesterol serum levels are only significantly lower in *AEBP1*^{-/-} males, not females (12). Collectively, these findings suggest that *AEBP1* may exert potent atherogenic effects *in vivo*. To investigate this possibility, proximal aortic cryosections obtained from young (12-wk) and old (32-wk), chow- and HFD-fed *AEBP1*^{TG}, *AEBP1*^{NT}, *AEBP1*^{+/+} and *AEBP1*^{-/-} mice were assessed for atherosclerotic lesion formation. Lesions were

Table 2. The effects of gender and age on atherosclerotic lesion size in *AEBP1^{TG}* mice fed an HFD.

Gender and genotype	Age (wks)	Total number of sections/mice (n)	Mean lesion area (%)
F <i>AEBP1^{TG}</i>	12	14/4	3.26 ± 0.55
M <i>AEBP1^{TG}</i>	12	15/4	3.09 ± 0.38
F <i>AEBP1^{NT}</i>	12	11/4	0.00 ± 0.00
M <i>AEBP1^{NT}</i>	12	11/4	0.00 ± 0.00
F <i>AEBP1^{TG}</i>	32	28/7	6.76 ± 0.88
M <i>AEBP1^{TG}</i>	32	15/4	3.00 ± 0.39
F <i>AEBP1^{NT}</i>	32	13/4	0.00 ± 0.00
M <i>AEBP1^{NT}</i>	32	12/3	0.00 ± 0.00

detected only in the HFD-fed *AEBP1^{TG}* mice (Table 1). Compared with *ApoE^{-/-}* and *LDLR^{-/-}* mice, HFD-fed *AEBP1^{TG}* mice develop relatively small, atypical atherosclerotic lesions that are surrounded by very thin, poorly characterized fibrous caps (Figures 1B, D). Additionally, lesions detected in *AEBP1^{TG}* mice are not continuous along the endothelial monolayer. Interestingly, although lesions are detected in both genders of *AEBP1^{TG}* mice, females develop lesions more prevalently (see Table 1) and of a larger mean area (Table 2).

***AEBP1* Ablation Reduces Atherosclerotic Lesion Area and Macrophage Infiltration into the Aortic Sinus**

Because *AEBP1^{-/-}* mice were raised on C57BL/6 background (12) and *AEBP1^{-/-}* macrophages exhibit enhanced cholesterol efflux and diminished inflammatory responsiveness (9), we anticipated that *AEBP1^{-/-}/ApoE^{-/-}* and *AEBP1^{-/-}/LDLR^{-/-}* double-knockout mice would be resistant to atherosclerotic lesion formation. Because of embryonic lethality in the *AEBP1^{-/-}/ApoE^{-/-}* double-knockout mice, we were only able to generate *AEBP1^{-/-}/LDLR^{-/-}* double-knockout mice. To assess the effect of *AEBP1* ablation on atherogenesis, groups of *AEBP1^{+/+}/LDLR^{-/-}* and *AEBP1^{-/-}/LDLR^{-/-}* littermates were placed on an atherogenic diet for 13 wks. Subsequently, atherosclerotic lesion formation was assessed by *en face* analysis (Figure 2A). Computational analysis revealed a significant reduction in lesion size in male (3.2-fold, $P = 0.001$;

3.9% versus 12.4% lesion area) and female (2.1-fold, $P = 0.0026$; 5.6% versus 11.8% lesion area) *AEBP1^{-/-}/LDLR^{-/-}* mice (Figure 2B). Consistently, histological analysis of the aortic roots revealed a remarkable attenuation of lesion formation in *AEBP1^{-/-}/LDLR^{-/-}* mice compared with *AEBP1^{+/+}/LDLR^{-/-}* littermates (Figure 2C). Quantification of lesion size revealed a significant decrease of lesion area in male (2.7-fold, $P = 0.0004$; 9.8% versus 26% lesion area) and female (1.7-fold, $P = 0.0126$; 19.5% versus 33.7%) *AEBP1^{-/-}/LDLR^{-/-}* mice compared with *AEBP1^{+/+}/LDLR^{-/-}* littermates (Figure 2D).

To experimentally address whether *AEBP1* deficiency causes impaired recruitment of monocytes into the developing lesions, we investigated the migration and homing of macrophages into the atherosclerotic lesions of *AEBP1^{-/-}/LDLR^{-/-}* mice. As shown in Figure 2E, homing of macrophages (F4/80) into the lesions was reduced in *AEBP1^{-/-}/LDLR^{-/-}* mice compared with *AEBP1^{+/+}/LDLR^{-/-}* controls. VCAM-1 is known to be crucial for monocyte extravasation into atherosclerotic lesions (16). Immunohistochemical analysis using rat anti-mouse CD106 primary antibody revealed that VCAM-1 expression is also reduced in the lesions of *AEBP1^{-/-}/LDLR^{-/-}* mice (see Figure 2E), suggesting that *AEBP1* ablation impairs macrophage infiltration into atherosclerotic lesions via the inhibition of VCAM-1 expression. It has been reported that advanced atherosclerotic lesions gradually accumulate T cells (17). Immunostaining of aortic sinus sections revealed a clear reduction in T-cell num-

bers (CD3) in the lesions of *AEBP1^{-/-}/LDLR^{-/-}* mice (see Figure 2E), indicating that *AEBP1* ablation also attenuates the accumulation of T cells in atherosclerotic lesions.

***AEBP1* Deficiency Influences Lipid and Energy Metabolism in *LDLR^{-/-}* Mice**

Interestingly, the attenuation of lesion formation in *AEBP1^{-/-}/LDLR^{-/-}* mice occurred in the absence of a significant change in serum lipid profile, except for plasma cholesterol levels, which were significantly ($P = 0.034$) lower in *AEBP1^{-/-}/LDLR^{-/-}* females than in the *AEBP1^{+/+}/LDLR^{-/-}* counterparts (Figure 3A). Although plasma triglyceride levels were lower in *AEBP1^{-/-}/LDLR^{-/-}* mice than in *AEBP1^{+/+}/LDLR^{-/-}* controls for both genders (1.49-fold in males and 1.37-fold in females), this difference did not reach statistical significance. We have previously reported that *AEBP1^{-/-}* mice display resistance to diet-induced obesity and reduction in adipose tissue mass (12). Weekly body weight measurement showed that the starting body weight of *AEBP1^{-/-}/LDLR^{-/-}* mice was also lower than that of *AEBP1^{+/+}/LDLR^{-/-}* mice and that the difference in body weight was maintained over the course of the experiment (Figure 3B). However, energy intake was not significantly different between *AEBP1^{-/-}/LDLR^{-/-}* and *AEBP1^{+/+}/LDLR^{-/-}* males (Figure 3C), despite the significant ($P = 0.004$) reduction in feed efficiency of those males (Figure 3D). Although *AEBP1^{-/-}/LDLR^{-/-}* females display significantly ($P = 0.006$) increased energy intake (see Figure 3C), their body weight values were slightly, but not significantly, reduced (see Figure 3D). Taken together, these results demonstrate that *AEBP1* ablation not only attenuates atherosclerotic lesion development *in vivo*, but also possibly influences lipid and energy metabolism.

BM-Derived *AEBP1* Is Critical in Atherogenesis

We have previously shown that *AEBP1* plays a key functional role in modulating *in vivo* adiposity and energy metabolism

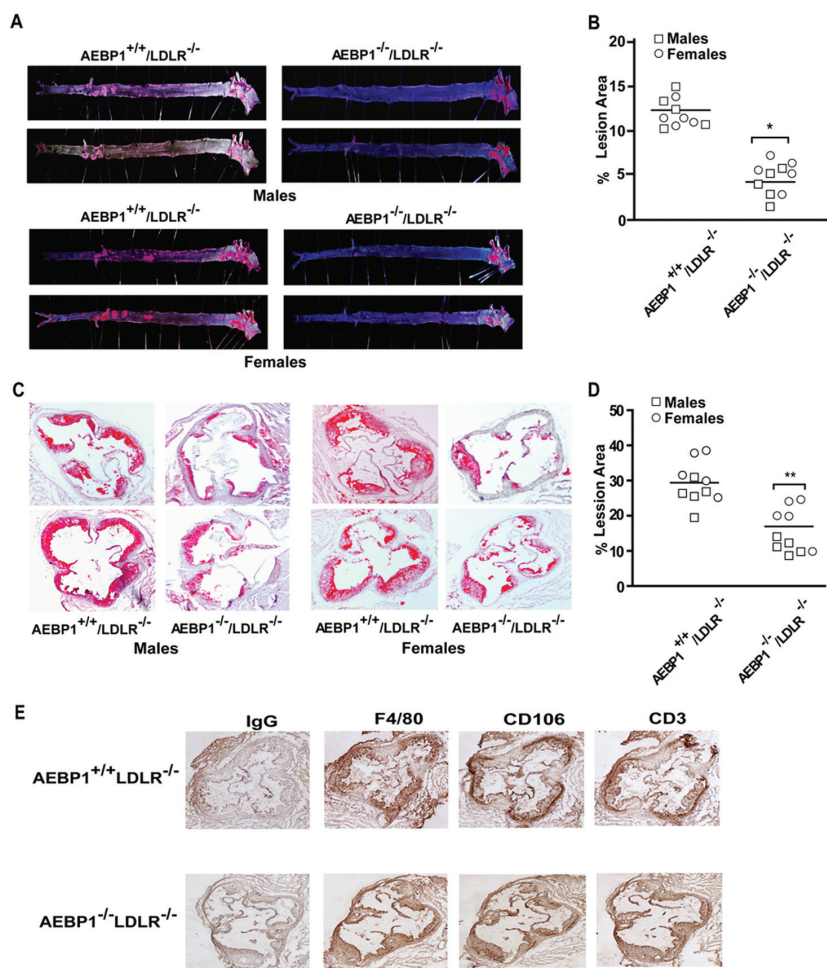


Figure 2. Ablation of *AEBP1* attenuates atherosclerosis in *LDLR*-null mice. (A) *En face* staining of aortas of *AEBP1*^{+/+}/*LDLR*^{-/-} and *AEBP1*^{-/-}/*LDLR*^{-/-} male and female mice. Mice were fed an atherogenic diet for 13 wks, and aortic lesion was analyzed *en face* with sudan IV staining. (B) Graphs showing quantification of atherosclerotic lesion size as a percentage of total aortic area. Error bars represent SEM, ***P* ≤ 0.001 (*n* = 5 males, *P* = 0.001), **P* ≤ 0.05 (*n* = 5 females, *P* = 0.0026). (C) Cross-sectional analysis at the aortic root of samples isolated from *AEBP1*^{+/+}/*LDLR*^{-/-} and *AEBP1*^{-/-}/*LDLR*^{-/-} mice. Representative ORO staining in the aortic sinus after 13 wks on the atherogenic diet. (D) Graphs showing quantification of atherosclerotic lesion size at the aortic sinus as a percentage of total aortic root area. Error bars represent SEM, ***P* ≤ 0.001 (*n* = 5 males, *P* = 0.0004), **P* ≤ 0.05 (*n* = 5 females, *P* = 0.0126). (E) Immunohistochemical analysis of the aortic atherosclerotic lesion (females) at low magnification (40×). Tissue sections obtained from aortic atherosclerotic lesion were treated with normal rat IgG, rat anti-mouse F4/80 (macrophage), rat anti-mouse CD106 (VCAM-1) and rat anti-mouse CD3 (T cells).

(12,13). Experimental evidence suggesting that adipose tissue pathophysiology (often exacerbated by obesity) strongly correlates with atherosclerosis is overwhelming (18). Although *AEBP1*^{-/-}/*LDLR*^{-/-} mice displayed significant resistance to atherosclerotic lesion development (Figure 2), the results may be due

to a compound effect of global, systemic disruption of *AEBP1* in these mice. To address this issue, chimeric mice were generated by BM transplantation to enable investigation of a direct and specific role of macrophage *AEBP1* in atherogenesis. To examine whether attenuation of atherosclerosis in *AEBP1*^{-/-}/*LDLR*^{-/-} mice

is macrophage-driven and not systemic, we transplanted *AEBP1*^{-/-}/*LDLR*^{-/-} BM cells into γ -irradiated *LDLR*^{-/-} mice. Because *AEBP1*^{-/-} macrophages exhibit enhanced cholesterol efflux and diminished inflammatory responsiveness (9–11), we anticipated that transplantation of BM cells from *AEBP1*^{-/-}/*LDLR*^{-/-} mice into *LDLR*^{-/-} mice would result in amelioration or attenuation of atherogenesis. Female *LDLR*^{-/-} recipients were reconstituted with male *AEBP1*^{-/-}/*LDLR*^{-/-} or *AEBP1*^{+/+}/*LDLR*^{-/-} BM cells, whereas male *LDLR*^{-/-} recipients were reconstituted with female *AEBP1*^{-/-}/*LDLR*^{-/-} or *AEBP1*^{+/+}/*LDLR*^{-/-} BM cells (Figure 4A). Sixteen weeks after transplantation, genomic DNA from BM cells was extracted and the engraftment of donor cells was confirmed by real-time PCR analysis of the *sex-determining region Y (SRY)* gene in the Y chromosome. *En face* analysis shows that the lesion area in *LDLR*^{-/-} mice that received *AEBP1*^{-/-}/*LDLR*^{-/-} BM cells (*LDLR*^{-/-}/*KO*-BM chimera) is significantly reduced compared with control mice (*LDLR*^{-/-}/*WT*-BM chimera) that received *AEBP1*^{+/+}/*LDLR*^{-/-} BM cells (2.0-fold, *P* = 0.0268) (Figure 4B). Consistently, aortic root sections stained with oil red O (ORO) also revealed reduced (1.7-fold, *P* = 0.05) accumulation of lipid deposits in the aortas of *LDLR*^{-/-}/*KO*-BM mice compared with the control mice *LDLR*^{-/-}/*WT*-BM (Figure 4C). Interestingly, the attenuation of atherosclerotic lesion formation in *LDLR*^{-/-}/*KO*-BM occurred in the absence of a significant change in plasma cholesterol levels (Figure 4D); however, triglyceride levels (Figure 4E) were significantly (*P* = 0.006) reduced in *LDLR*^{-/-}/*KO*-BM mice compared with the control mice *LDLR*^{-/-}/*WT*-BM.

To further confirm that macrophage *AEBP1* plays a critical role in the development of atherosclerosis, we generated more BM-chimeric mice, using the *ApoE*^{-/-} background mice, to enable investigation of a direct and specific role of macrophage *AEBP1* in atherosclerotic lesion formation. To this end, BM cells from *AEBP1*^{TG} mice were transplanted into γ -irradiated *ApoE*^{-/-} mice at the age of 10 wks. Female *ApoE*^{-/-}

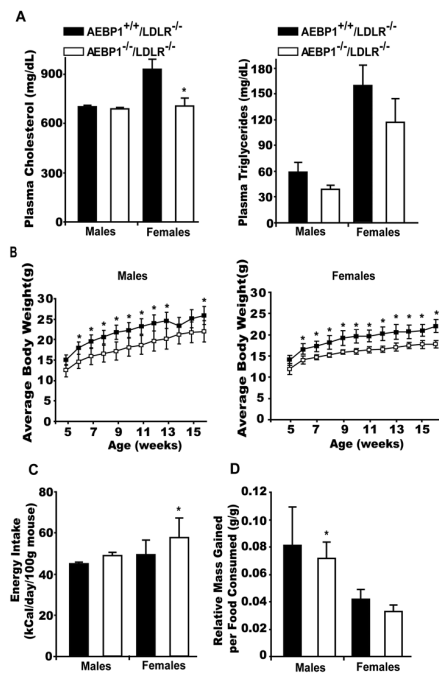


Figure 3. Ablation of *AEBP1* influence on lipid and energy metabolism in *LDLR*^{-/-} mice. (A) Plasma cholesterol levels of *AEBP1*^{+/+}/*LDLR*^{-/-} and *AEBP1*^{-/-}/*LDLR*^{-/-} mice after 13 wks of atherogenic diet feeding. Error bars represent SEM, **P* ≤ 0.05 (*n* = 4 males, *P* = 0.44; *n* = 5 females, *P* = 0.034). Plasma triglycerides levels of *AEBP1*^{+/+}/*LDLR*^{-/-} and *AEBP1*^{-/-}/*LDLR*^{-/-} mice after 13 wks of atherogenic diet feeding. Error bars represent SEM (*n* = 5 males, *P* = 0.26; *n* = 5 females, *P* = 0.28). (B) Measurement of body weight of *AEBP1*^{+/+}/*LDLR*^{-/-} and *AEBP1*^{-/-}/*LDLR*^{-/-} mice fed an atherogenic diet. Three-week-old mice were fed an atherogenic diet for 13 wks. Body weight was measured weekly. (C) Food intake was measured weekly and normalized to body weight. Total energy intake per group in a cage was calculated as the mean value per 100 g body weight. The data points represent the mean values of 13 weekly measurements of total energy intake. Error bars represent SEM, **P* ≤ 0.05 (*n* = 5 males, *P* = 0.377; *n* = 5 females, *P* = 0.006). (D) Feed efficiency was calculated with the weekly measurements of mean values of weight gain and food consumption. The data points represent the mean values of 13 weekly measurements of feed efficiency. Error bars represent SEM, **P* ≤ 0.05 (*n* = 5 males, *P* = 0.004; *n* = 5 females, *P* = 0.374).

recipients were reconstituted with male *AEBP1*^{TG} or *AEBP1*^{NT} BM cells, whereas male *ApoE*^{-/-} recipients were reconstituted with female *AEBP1*^{TG} or *AEBP1*^{NT} BM cells (Figure 5A). As expected, transplantation of *AEBP1*^{NT} macrophages with the normal *ApoE* gene into *ApoE*^{-/-} mice (*ApoE*^{-/-}/*NT-BM*) resulted in expression of ApoE (Figure 6C) and significant protection from diet-induced atherosclerosis. The extent of lesion in *ApoE*^{-/-}/*NT-BM* mice (<10%) (Figure 5B) is markedly less than the level normally seen in *ApoE*^{-/-} mice fed an atherogenic diet (>40%). In contrast, *en face* aorta analysis showed robust formation of atherosclerotic lesions in mice that received *AEBP1*^{TG} BM cells (*ApoE*^{-/-}/*TG-BM*) (see Figure 5B). Interestingly, male *ApoE*^{-/-}/*TG-BM* mice displayed slightly more advanced atherosclerotic lesions than their female counterparts (17.1% versus 12.9%). Male recipient *ApoE*^{-/-} mice had slightly enhanced atherosclerotic lesion formation than female recipient *ApoE*^{-/-} mice (2.5-fold, *P* = 0.0001, versus 1.8-fold, *P* = 0.0001) when transplanted with *AEBP1*^{TG} BM cells. Consistently, aortic root sections stained with ORO also revealed elevated accumulation of lipid deposits in the aortas of *ApoE*^{-/-}/*TG-BM* mice in a gender-influenced manner (4.7-fold, *P* = 0.0001, versus 3.0-fold, *P* = 0.0001) (Figure 5C). Notably, although transplantation of *AEBP1*^{TG} BM cells into *ApoE*^{-/-} mice led to a significant elevation of plasma cholesterol and triglyceride levels in male and female recipients (Figure 5D), this difference did not reach statistical significance, as in the case of *AEBP1*^{TG} males (Figure 1).

BM-Derived AEBP1 Promotes Atherosclerosis by Downregulating Cholesterol Efflux Mediators PPAR γ 1 and LXR α and Provoking Macrophage Inflammatory Responsiveness

We have previously shown that AEBP1 promotes foam cell formation by downregulating PPAR γ 1, LXR α and their downstream target genes (9,11). To examine whether AEBP1 modulates PPAR γ 1 and LXR α expression in macrophages of the chimeric mice, macrophage protein extracts were subjected to immunoblot-

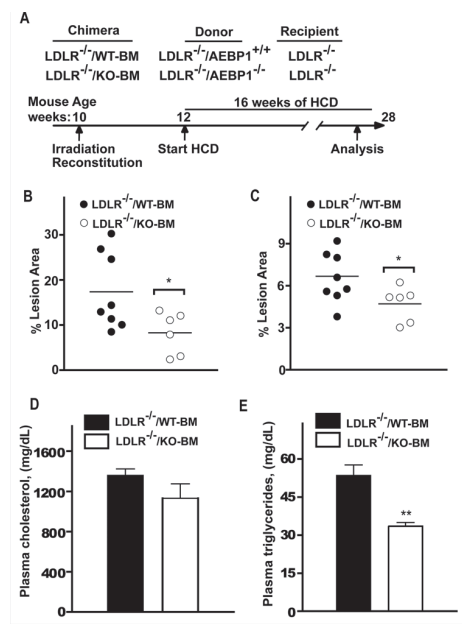


Figure 4. Atherogenesis is significantly attenuated in *LDLR*^{-/-}/*KO-BM* mice compared with *LDLR*^{-/-}/*WT-BM* mice. (A) Experimental design of generation of radiation chimera and list of chimeras. (B) *En face* analysis of aorta atherosclerotic lesion formation in *LDLR*^{-/-}/*WT-BM* (*n* = 8) and *LDLR*^{-/-}/*KO-BM* (*n* = 6) chimeras. Lipid staining was performed using the sudan IV reagent. Quantification of atherosclerotic lesion area was performed with ImageJ; the numbers represent atherosclerotic lesion as a percentage of total aorta area (**P* = 0.0268). (C) Quantification of atherosclerotic lesions of aortic roots in *LDLR*^{-/-}/*WT-BM* (*n* = 8) and *LDLR*^{-/-}/*KO-BM* (*n* = 6) chimeras. Atherosclerotic lesion size at the aortic sinus as a percentage of total aortic root area (**P* = 0.05) is shown. (D) Plasma cholesterol levels of *LDLR*^{-/-}/*WT-BM* (*n* = 8) and *LDLR*^{-/-}/*KO-BM* (*n* = 6) chimeras after 16 wks of atherogenic diet feeding. Error bars represent SEM (*P* = 0.07). (E) Plasma triglycerides levels of *LDLR*^{-/-}/*WT-BM* (*n* = 8) and *LDLR*^{-/-}/*KO-BM* (*n* = 6) chimeras after 16 wks of atherogenic diet feeding. Error bars represent SEM (***P* = 0.006).

ting (Figure 6A). Quantification analysis revealed more than a 3.0-fold (*P* = 0.0001) and 1.8-fold (*P* = 0.0001) decrease in protein levels of PPAR γ 1 and LXR α , respectively, in *ApoE*^{-/-}/*TG-BM* macrophages (Figure 6B). Similarly, real-time PCR analysis revealed that transplantation of

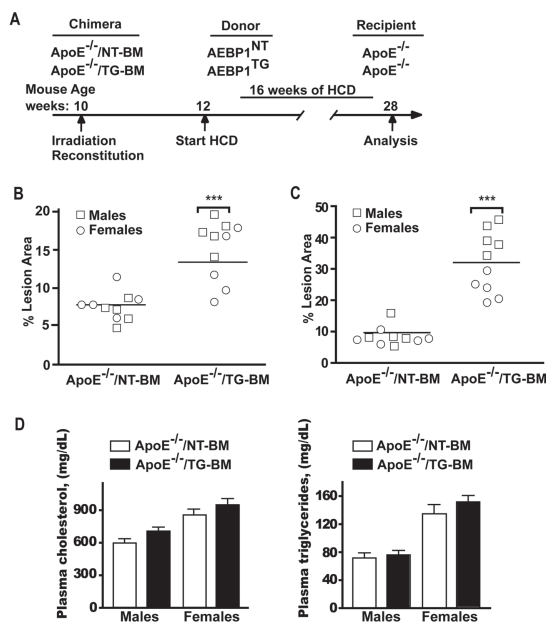


Figure 5. Atherogenesis is significantly accelerated in *ApoE*^{-/-}/*TG-BM* mice compared with *ApoE*^{-/-}/*NT-BM* mice. (A) Experimental design of generation of radiation chimera and list of chimeras (n = 5) for each chimera. (B) *En face* analysis of aorta atherosclerotic lesion formation in *ApoE*^{-/-}/*NT-BM* and *ApoE*^{-/-}/*TG-BM* chimeras. Lipid staining was performed using sudan IV reagent. Quantification of atherosclerotic lesion area was performed with ImageJ; numbers represent the atherosclerotic lesion as a percentage of total aorta area (****P* = 0.0001). (C) ORO staining of atherosclerotic lesions of aortic roots in *ApoE*^{-/-}/*NT-BM* and *ApoE*^{-/-}/*TG-BM* chimeras. Graphs showing quantification of atherosclerotic lesion size at the aortic sinus as a percentage of total aortic root area (****P* = 0.0001). (D) Analysis of total plasma cholesterol and triglyceride levels in *ApoE*^{-/-}/*NT-BM* and *ApoE*^{-/-}/*TG-BM* chimeras.

AEBP1^{TG} BM cells into *ApoE*^{-/-} mice leads to a 2.7-fold (*P* = 0.0001) reduction in PPARγ1 levels in *ApoE*^{-/-}/*TG-BM* macrophages compared with *ApoE*^{-/-}/*NT-BM* control macrophages (Figure 6C). Moreover, the expression of major cholesterol efflux mediators (ApoE, ABCA1 and ABCG1, which are downstream target genes of PPARγ1 and LXRα) was significantly reduced (2.8-, 1.4- and 1.5-fold, respectively) in *ApoE*^{-/-}/*TG-BM* macrophages compared with *ApoE*^{-/-}/*NT-BM* control macrophages (see Figure 6C).

Proinflammatory cytokines have been implicated as key mediators in atherogenesis. We have previously shown that *AEBP1* overexpression in macrophages is accompanied by a significant increase in the production of major proinflammatory mediators including IL-6 and tumor necrosis factor (TNF)-α (9). Here, the expression of IL-6 and TNF-α was examined in the

macrophages of BM-chimeric *ApoE*^{-/-} mice. As shown in Figure 6C, IL-6 and TNF-α levels were significantly (*P* = 0.0001) elevated (1.8- and 1.6-fold, respectively) in *ApoE*^{-/-}/*TG-BM* macrophages compared with *ApoE*^{-/-}/*NT-BM* control macrophages. Taken together, these results strongly suggest that macrophage *AEBP1* exerts a potent pro-atherogenic function *in vivo*.

DISCUSSION

It has been well established that mice are particularly resistant to the formation of atherosclerotic lesions (19,20). Even when fed a HCD (100 times their normal daily intake), mice do not show signs of atherogenesis (21). Nevertheless, two widely recognized genetically altered mouse models exist that spontaneously develop lesions; *ApoE*^{-/-} mice fed a standard diet (22,23) and *LDLR*^{-/-} mice fed a HCD (24). In this study, we identify

AEBP1^{TG} mice as a novel murine model of atherosclerosis. *AEBP1*^{TG} mice develop relatively small, atypical atherosclerotic lesions that are surrounded by very thin, poorly characterized fibrous caps, and the lesions are not continuous along the endothelial monolayer. These results may be due to differential athero-susceptibility by different strains of mice (25–27). *AEBP1*^{TG} mice were raised on the FVB/N background, whereas *ApoE*^{-/-} and *LDLR*^{-/-} mice were raised on the C57BL/6 background. It is documented that the mean lesion area is 3.5- to 9-fold higher in *ApoE*^{-/-} mice raised on the C57BL/6 background, compared with *ApoE*^{-/-} mice raised on the FVB/N background (26). The fact that FVB/N mice are relatively athero-resistant coupled with the high athero-susceptibility exhibited by *AEBP1*^{TG} mice reflects the robust atherogenic potential of *AEBP1*. Here, a number of points are noteworthy. First, no atherosclerotic lesions are detected in chow diet-fed *AEBP1*^{TG} mice, suggesting that *AEBP1*^{TG} mice resemble *LDLR*^{-/-} mice with regard to their ability to form lesions in a diet-induced manner. Interestingly, *AEBP1* expression is induced in the macrophages of mice fed an HFD (A Majdalawieh and H-S Ro, unpublished observations). We have previously shown that *AEBP1* expression is also induced in the adipose tissues of mice fed an HFD (13). These results suggest that a critical level of *AEBP1* is necessary for the lesion formation in *AEBP1*^{TG} mice. Second, although lesions are detected in both genders of *AEBP1*^{TG} mice, females develop lesions more prevalently (see Table 1) and of a larger mean area (see Table 2). Despite the low number of samples used, these data are consistent with other studies suggesting that HFD-fed female mice are more susceptible to lesion formation compared with HFD-fed male mice (27–30). Several explanations were provided to account for gender-specific differences with regard to athero-susceptibility (27–32). The only satisfactory explanation for the gender-specific, athero-susceptibility differences in *AEBP1*^{TG} mice is that *AEBP1*^{TG} females,

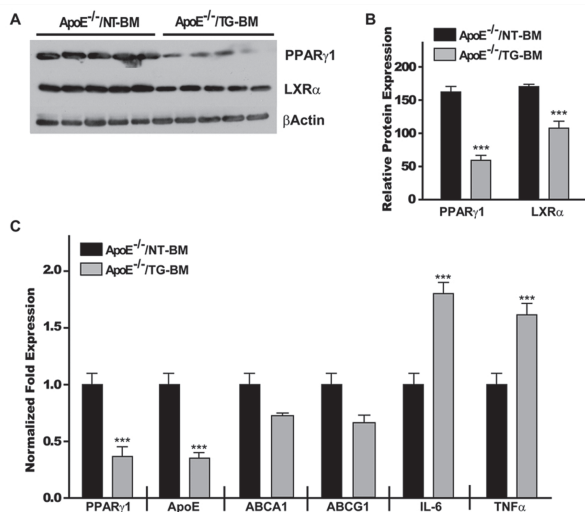


Figure 6. PPAR γ 1 and LXR α expression and proinflammatory mediators are significantly up-regulated in *ApoE*^{-/-}/TG-BM macrophages compared with *ApoE*^{-/-}/NT-BM macrophages. (A) Relative protein levels of PPAR γ 1 and LXR α in macrophages from chimeras were analyzed by immunoblotting with specific antibodies. (B) Densitometric analysis on the basis of β -actin expression in macrophage from chimeras is shown. (C) Transcript levels of PPAR γ 1, ApoE, IL-6 and TNF- α were assessed by real-time PCR analysis. Statistical significance was determined relative to protein expression level or mRNA level in macrophages isolated from *ApoE*^{-/-}/NT-BM mice (n = 5). Transcript levels of ABCA1 and ABCG1 were assessed by real-time PCR analysis in triplicate with pooled samples (n = 5). ****P* < 0.001.

but not males, have significantly elevated cholesterol and triglyceride serum levels compared with their *AEBP1*^{NT} counterparts (Figure 1A). This gender-specific effect is most unlikely due to alteration of sex hormones in the *AEBP1*^{TG} females, in which assessment of serum estrogen levels did not reveal any significant difference between *AEBP1*^{TG} females and *AEBP1*^{NT} counterparts (unpublished observations).

Many studies have demonstrated that promotion or inhibition of atherosclerosis is not always preceded or accompanied by changes in the plasma lipoprotein profile (31,33,34). Here, it is important to emphasize that atherosclerosis can be initiated and advanced despite normal plasma lipoprotein profile. Interestingly, *AEBP1*^{TG} males, which have plasma cholesterol and triglyceride levels that are statistically comparable to their *AEBP1*^{NT} male counterparts (see Figure 1A), clearly develop atherosclerotic lesions (see Table 1). Hence, these findings lend support to the inflammatory aspect of atherosclerosis, which can develop de-

spite normal plasma lipoprotein profile. Interestingly, *AEBP1*^{TG} mice seem to be relatively resistant to elevated cholesterol levels upon HFD challenge. Whereas HFD-fed *ApoE*^{-/-} and *LDLR*^{-/-} mice display approximately six-fold elevation in plasma cholesterol levels (1,800 and 1,500 mg/dL, respectively), HFD-fed *AEBP1*^{TG} females have less than two-fold elevated cholesterol levels than their HFD-fed *AEBP1*^{NT} counterparts (see Figure 1A). So, *AEBP1*^{TG} mice may serve as a preferred *in vivo* model to elucidate the inflammatory events during atherosclerosis in the absence of severe hyperlipidemia.

Macrophages isolated from *AEBP1*^{TG} males express significantly higher levels of IL-6, TNF- α , monocyte chemoattractant protein 1 (MCP-1) and inducible nitric oxide synthase (iNOS) than macrophages isolated from *AEBP1*^{NT} mice (9), confirming that inflammation is a critical event in atherosclerosis. In fact, there is a general consensus among researchers that hyperlipidemia is not sufficient on its own to lead to the development of advanced atherosclerotic lesions and that inflammatory

events such as monocyte recruitment, macrophage activation, cytokine and chemokine production and infiltration of other immune cells (for example, T cells, neutrophils and mast cells) are critical for atherosclerotic lesion initiation and progression. Interestingly, *AEBP1* ablation reduces atherosclerotic lesion area and causes reduction of T-cell number in *LDLR*^{-/-} mice (see Figure 2). It has been previously shown that infiltration of T cells into the atherosclerotic lesions is a crucial event in the early phase of atherogenesis, and as the disease progresses, macrophage recruitment and activation intensify and macrophages become the predominant cell type during the late phase of atherosclerosis (35–38). It is interesting to speculate that *AEBP1* is not only important in controlling macrophage infiltration during the late phase of atherogenesis, but it may also be critically involved in the early phase of the disease.

To enable investigation of a potential direct and specific role of *AEBP1* in atherogenesis, we generated *AEBP1*^{TG}/*LDLR*^{-/-} hybrid mice. However, atherosclerotic lesion analysis in the hybrid mice did not yield any meaningful results, possibly because of the mixed-strain effect on atherosclerotic lesion development in the hybrid mice. To avoid the strain effect, we generated *AEBP1*^{-/-}/*LDLR*^{-/-} double-knockout mice on the same C57BL/6 background. These double-knockout mice exhibited significant resistance to atherosclerotic lesion development compared with the control *AEBP1*^{+/+}/*LDLR*^{-/-} mice (see Figure 2). However, this may be due to a compound effect of global disruption of *AEBP1* in the double-knockout mice (see Figure 3). To definitively evaluate the functional role of *AEBP1* signaling in atherogenesis and to investigate a direct role of macrophage *AEBP1* in the development of atherosclerosis, we also generated chimeric mice by BM transplantation. Experimental evidence suggests that while transplantation of *AEBP1*^{-/-} BM cells into *LDLR*^{-/-} recipients attenuates lesion formation (see Figure 4), transplantation of *AEBP1*^{TG} BM cells into *ApoE*^{-/-} re-

cipts enhances lesion formation (see Figure 5) by downregulating cholesterol efflux mediators PPAR γ 1 and LXR α and provoking macrophage inflammatory responsiveness (see Figure 6). Our findings strongly suggest that macrophage AEBP1 plays a critical role in the development of atherosclerosis. The potential pro-atherogenic properties of AEBP1 may be a byproduct of a vital interplay of its ability to antagonize PPAR γ 1 and LXR α cholesterol efflux functions in macrophages and its ability to promote inflammation via enhanced NF- κ B transcriptional activity (39,40). We anticipate that AEBP1 may serve as a molecular candidate toward the development of therapeutic strategies to ameliorate or attenuate atherogenesis.

ACKNOWLEDGMENTS

We thank Chris Webber, Janette Fleming, Debby Currie and Patricia Colp for their technical assistance. This work was supported by a grant from the Canadian Institutes of Health Research (to H-S Ro).

DISCLOSURE

The authors declare that they have no competing interests as defined by *Molecular Medicine*, or other interests that might be perceived to influence the results and discussion reported in this paper.

REFERENCES

1. Ross R. (1999) Atherosclerosis: an inflammatory disease. *N. Engl. J. Med.* 340:115–26.
2. Libby P. (2002) Inflammation in atherosclerosis. *Nature.* 420:868–74.
3. Ricote M, et al. (1998) Expression of the peroxisome proliferator-activated receptor gamma (PPARgamma) in human atherosclerosis and regulation in macrophages by colony stimulating factors and oxidized low density lipoprotein. *Proc. Natl. Acad. Sci. U. S. A.* 95:7614–9.
4. Tontonoz P, Nagy L, Alvarez JG, Thomazy VA, Evans RM. (1998) PPARgamma promotes monocyte/macrophage differentiation and uptake of oxidized LDL. *Cell.* 93:241–52.
5. Nagy L, Tontonoz P, Alvarez JG, Chen H, Evans RM. (1998) Oxidized LDL regulates macrophage gene expression through ligand activation of PPARgamma. *Cell.* 93:229–40.
6. Venkateswaran A, et al. (2000) Control of cellular cholesterol efflux by the nuclear oxysterol receptor LXR alpha. *Proc. Natl. Acad. Sci. U. S. A.* 97:12097–102.
7. Chawla A, et al. (2001) A PPAR gamma-LXR-

- ABCA1 pathway in macrophages is involved in cholesterol efflux and atherogenesis. *Mol. Cell.* 7:161–71.
8. Ro H-S, Kim SW, Wu D, Webber C, Nicholson TE. (2001) Gene structure and expression of the mouse adipocyte enhancer-binding protein. *Gene.* 280:123–33.
9. Majdalawieh A, Zhang L, Fuki IV, Rader DJ, Ro H-S. (2006) Adipocyte enhancer-binding protein 1 is a potential novel atherogenic factor involved in macrophage cholesterol homeostasis and inflammation. *Proc. Natl. Acad. Sci. U. S. A.* 103:2346–51.
10. Majdalawieh A, Zhang L, Ro H-S. (2007) Adipocyte enhancer-binding protein-1 promotes macrophage inflammatory responsiveness by up-regulating NF-kappaB via IkappaBalpha negative regulation. *Mol. Biol. Cell.* 18:930–42.
11. Majdalawieh A, Ro H-S. (2009) LPS-induced suppression of macrophage cholesterol efflux is mediated by adipocyte enhancer-binding protein 1. *Int. J. Biochem. Cell. Biol.* 41:1518–25.
12. Ro H-S, et al. (2007) Adipocyte enhancer-binding protein 1 modulates adiposity and energy homeostasis. *Obesity.* 15:288–302.
13. Zhang L, et al. (2005) The role of AEBP1 in sex-specific diet-induced obesity. *Mol. Med.* 11:39–47.
14. Palinski W, et al. (1994) ApoE-deficient mice are a model of lipoprotein oxidation in atherogenesis: demonstration of oxidation-specific epitopes in lesions and high titers of autoantibodies to malondialdehyde-lysine in serum. *Arterioscler. Thromb.* 14:605–16.
15. Boisvert WA, Santiago R, Curtiss LK, Terkeltaub RA. (1998) A leukocyte homologue of the IL-8 receptor CXCR-2 mediates the accumulation of macrophages in atherosclerotic lesions of LDL receptor-deficient mice. *J. Clin. Invest.* 101:353–63.
16. Cybulsky MI, et al. (2001) A major role for VCAM-1, but not ICAM-1, in early atherosclerosis. *J. Clin. Invest.* 107:1255–62.
17. Zhou X, Stemme S, Hansson GK. (1996) Evidence for a local immune response in atherosclerosis: CD4+ T cells infiltrate lesions of apolipoprotein-E-deficient mice. *Am. J. Pathol.* 149:359–66.
18. Bays HE. (2009) “Sick Fat,” metabolic disease, and atherosclerosis. *Am. J. Med.* 122:S26–37.
19. Zhang SH, Reddick RL, Piedrahita JA, Maeda N. (1992) Spontaneous hypercholesterolemia and arterial lesions in mice lacking apolipoprotein E. *Science.* 258:468–71.
20. Breslow JL. (1996) Mouse models of atherosclerosis. *Science.* 272:685–8.
21. Reardon CA, Getz GS. (2001) Mouse models of atherosclerosis. *Curr. Opin. Lipidol.* 12:167–73.
22. Piedrahita JA, Zhang SH, Hageman JR, Oliver PM, Maeda N. (1992) Generation of mice carrying a mutant apolipoprotein E gene inactivated by gene targeting in embryonic stem cells. *Proc. Natl. Acad. Sci. U. S. A.* 89:4471–5.
23. Plump AS, et al. (1992) Severe hypercholesterolemia and atherosclerosis in apolipoprotein E-deficient mice created by homologous recombination in ES cells. *Cell.* 71:343–53.
24. Ishibashi S, et al. (1993) Hypercholesterolemia in

- low density lipoprotein receptor knockout mice and its reversal by adenovirus-mediated gene delivery. *J. Clin. Invest.* 92:883–93.
25. Paigen B, Mitchell D, Holmes PA, Albee D. (1987) Genetic analysis of strains C57BL/6J and BALB/cJ for Ath-1, a gene determining atherosclerosis susceptibility in mice. *Biochem. Genet.* 25:881–92.
26. Dansky HM, et al. (1999) Genetic background determines the extent of atherosclerosis in ApoE-deficient mice. *Arterioscler. Thromb. Vasc. Biol.* 19:1960–8.
27. Smith JD, et al. (2003) In silico quantitative trait locus map for atherosclerosis susceptibility in apolipoprotein E-deficient mice. *Arterioscler. Thromb. Vasc. Biol.* 23:117–22.
28. Paigen B, Holmes PA, Mitchell D, Albee D. (1987) Comparison of atherosclerotic lesions and HDL-lipid levels in male, female, and testosterone-treated female mice from strains C57BL/6, BALB/c, and C3H. *Atherosclerosis.* 64:215–21.
29. Paigen B, Morrow A, Holmes PA, Mitchell D, Williams RA. (1987) Quantitative assessment of atherosclerotic lesions in mice. *Atherosclerosis.* 68:231–40.
30. Ishii I, Ito Y, Morisaki N, Saito Y, Hirose S. (1995) Genetic differences of lipid metabolism in macrophages from C57BL/6J and C3H/HeN mice. *Arterioscler. Thromb. Vasc. Biol.* 15:1189–94.
31. Song C, Hiipakka RA, Liao S. (2001) Auto-oxidized cholesterol sulfates are antagonistic ligands of liver X receptors: implications for the development and treatment of atherosclerosis. *Steroids.* 66:473–9.
32. Smith JD, Dansky HM, Breslow JL. (2001) Genetic modifiers of atherosclerosis in mice. *Ann. N.Y. Acad. Sci.* 947:247–53.
33. Gu L, et al. (1998) Absence of monocyte chemoattractant protein-1 reduces atherosclerosis in low density lipoprotein receptor-deficient mice. *Mol. Cell.* 2:275–81.
34. Tsukamoto K, et al. (2000) Hepatic expression of apolipoprotein E inhibits progression of atherosclerosis without reducing cholesterol levels in LDL receptor-deficient mice. *Mol. Ther.* 1:189–94.
35. Song L, Leung C, Schindler C. (2001) Lymphocytes are important in early atherosclerosis. *J. Clin. Invest.* 108:251–9.
36. Roselaar SE, Kakkannathu PX, Daugherty A. (1996) Lymphocyte populations in atherosclerotic lesions of apoE^{-/-} and LDL receptor^{-/-} mice: decreasing density with disease progression. *Arterioscler. Thromb. Vasc. Biol.* 16:1013–8.
37. Zhou X, Nicoletti A, Elhage R, Hansson GK. (2000) Transfer of CD4(+) T cells aggravates atherosclerosis in immunodeficient apolipoprotein E knockout mice. *Circulation.* 102:2919–22.
38. Hansson GK, Hermansson A. (2011) The immune system in atherosclerosis. *Nat. Immunol.* 12:204–12.
39. Majdalawieh A, Ro HS. (2010) PPARgamma1 and LXRalpha face a new regulator of macrophage cholesterol homeostasis and inflammatory responsiveness, AEBP1. *Nucl. Recept. Signal.* 8:e004.
40. Majdalawieh A, Ro HS. (2010) Regulation of IkappaBalpha function and NF-kappaB signaling: AEBP1 is a novel proinflammatory mediator in macrophages. *Mediators Inflamm.* 2010:823821.